Photochemistry and Spectroscopy of Monosubstituted Derivatives of Tungsten Hexacarbonyl Which Exhibit Low-Efficiency Photoreactivities[1]

R. Marc Dahlgren[2] and Jeffrey I. Zink*[3]

Contribution from the Department of Chemistry, University of California, Los Angeles, California 90024. *Received August 13, 1978*

Abstract: The photochemistry and electronic and infrared spectroscopy of $W(CO)_5X$, X = Cl^-, Br^-, I^-, NCO^-, and CS, are reported. The lowest energy excited state of the latter compound is metal to ligand charge transfer as shown by magnetic circular dichroism spectroscopy. The lowest excited state of the anions is primarily ligand field. The low photoreactivity ($\phi < 0.1$) of all of these compounds is interpreted in terms of excited state bonding properties. The previously proposed classification of low reactivity excited state origins is expanded to include both ligand-field and charge-transfer states.

The modes and efficiencies of ligand substitution[4] and internal ligand phototransformation processes[5] arising from population of the lowest energy excited state of $W(CO)_5L$ complexes have been classified within three reactivity patterns. Class 1 photochemistry, which was characteristic of the amine derivatives of $W(CO)_6$, was defined as low-efficiency carbonyl photosubstitution with high-efficiency metal–ammine dissociative photolabilization. Class 2 photochemistry, characteristic of phosphorus donor derivatives, consisted of high quantum yields for both metal–L and metal–CO substitution. Finally, class 3 reactivity was defined as low-efficiency photolabilization of all metal–ligand bonds. This third classification is the subject of this paper.

Class 3 photochemistry was originally observed for the bromide, thiocarbonyl, methylmethoxycarbene, phenylmethoxycarbene,[4] azide,[5] and substituted pyridine derivatives[6] of tungsten hexacarbonyl. All of these complexes exhibited quantum yields of $\leq 10^{-2}$ for both unique ligand and carbonyl photosubstitution from the lowest energy excited state. These results contrasted to yields of 0.1–0.6 for unique ligand substitution in both the class 1 and 2 materials.[4,7,8] The halide and pseudohalide derivatives of $W(CO)_6$ which are investigated in this work ($W(CO)_5L$ (L = Cl^-, Br^-, I^-, and NCO^-)) were chosen with the objective of establishing the generality of this reactivity classification first observed for the bromide material. A detailed investigation was warranted because the reported photochemistry of closely related derivatives $W(Cp)(CO)_3X$[9] and $Re(CO)_5X$[11] (X = halide), which consisted of efficient carbon monoxide loss with little halide substitution, was quite different from the photochemistry of $W(CO)_5Br^-$.[4]

We report here the results of spectroscopic and photochemical analyses of class 3 substituted tungsten carbonyl complexes. It is shown that there are two subclassifications within the general class 3 reactivity pattern. The lowest energy excited states are assigned using spectroscopic and electrochemical techniques. Finally, a bonding model is developed to explain the photochemistry of these materials.

Results

1. Spectroscopy. Electronic Absorption and Magnetic Circular Dichroism Spectra. The low-energy region of the electronic absorption spectrum of $W(CO)_5L$, where L = CS, $C(CH_3)(OCH_3)$, $C(Ph)(OCH_3)$, Cl^-, Br^-, I^- and NCO^-, is dominated by a single intense band ($\epsilon \sim 500$–3200 L/mol·cm) at about 2.5 μm^{-1} with a weak red shoulder at about 2.2 μm^{-1}. The energies of these bands are given in Table I. Representative examples of magnetic circular dichroism (MCD) spectra of these low-energy electronic absorptions of two representative class 3 compounds ($W(CO)_5Br^-$ and $W(CO)_5CS$) are shown in Figures 1 and 2.[12,13]

An MCD *A* term of positive sense is associated with the major low-energy electronic transition of $W(CO)_5Br^-$ in Figure 1. The lower energy feature in the MCD, which may be either another *A* term or two oppositely signed *B* terms, occurs in the region of the red shoulder in the optical spectrum. The MCD spectra for the other anionic $W(CO)_5X^-$ derivatives are extremely similar to that of $W(CO)_5Br^-$ in Figure 1.

The low-intensity, low-energy feature in the electronic spectrum of $W(CO)_5CS$ (Figure 2) demonstrates little if any hypsochromic shift upon increasing the solvent dielectric strength. The MCD of the complex does not contain a positive *A* term as observed for the bromide derivative. Instead, two oppositely signed *B* terms are observed corresponding to the major peak at 2.39 μm^{-1} and the small red shoulder of the peak at 2.25 μm^{-1}. The separation of these peaks in the MCD precludes an *A*-term assignment.

Luminescence Spectroscopy. The halide and pseudohalide derivatives luminesce in the region of 520 nm when excited at 400 nm in 77 K glasses similar to the emission observed for the class 1 and 2 materials.[4,14] Table II contains the luminescence energy, bandwidth, and lifetime data for these materials. Emission from the thiocarbonyl and carbene complexes could not be detected under similar conditions. The emission maximum changes by only 0.22 μm^{-1} as the unique ligand is varied. The lifetimes of these complexes are intermediate between those obtained for class 1 and 2 derivatives (~ 1 μs)[14] and those reported for the substituted pyridine derivatives (~ 30 μs).[6] The quantum yields for emission at 77 K have been determined for 390-nm excitation of three complexes ($[NEt_4][W(CO)_5Br]$ in a 4:1 EtOH–MeOH glass, $[AsPh_4][W(CO)_5Br]$ in the same glass, and $W(CO)_5(py)$ in 2-MeTHF), and are identically $2 \times 10^{-2} \pm 20\%$.

Infrared Spectroscopy. The force constants for the carbon–oxygen stretching vibrations have been determined utilizing the Cotton–Kraihanzel approximation,[15] and are given in Table III. Graham $\Delta\sigma$ and $\Delta\pi$ values have also been obtained[16] and are included in this table. $W(CO)_5$(cyclohexylamine) was used as the reference compound with $\Delta\sigma = \Delta\pi = 0$. The relative values of $\Delta\sigma$ and $\Delta\pi$ indicate that the halide and pseudohalide ligands are π accepting and poorer σ donating compared to cyclohexylamine while the carbene and CS ligands are strong π acceptors and equal or better σ donors. Therefore, these latter molecules are stronger overall ligands than simple amines while the halides and pseudohalides, hereafter called "halides", are weaker ligands.

2. Electrochemistry. Cyclic voltammograms were obtained for $W(CO)_5X^-$ (X = Br, I, and NCO). A clean oxidation is noted at about +0.6 V which is irreversible as evidenced by the lack of symmetry of the cyclic plot (i.e., the corresponding reduction is not well resolved). Applying a potential larger than

0002-7863/79/1501-1448$01.00/0

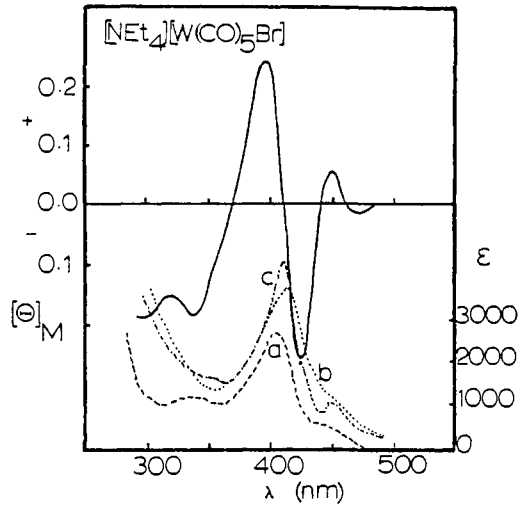

Figure 1. Optical and magnetic circular dichroism spectra of $[NEt_4][W(CO)_5Br]$: (a) MCD and optical spectra in 1,2-dichloroethane at 300 K; (b) in EPA at 300 K; (c) in EPA at 77 K (uncorrected for volume contractions).

Table I. Energies of the Electronic Spectral Features of $W(CO)_5L$ Complexes

$W(CO)_5L$ L	major band, μm^{-1}	red shoulder, μm^{-1}
Cl^- [a]	2.49	2.18
Br^- [a]	2.44	2.21
I^- [a]	2.48	2.25
NCO^- [a]	2.50	2.22
CS[b]	2.39	2.25
$C(CH_3)(OCH_3)$[b]	2.20[c]	
$C(Ph)(OCH_3)$[b]	1.94[c]	

[a] $CHCl_3$ solvent. [b] Cyclohexane solvent; taken from ref 4. [c] Only a single low-energy band was resolved.

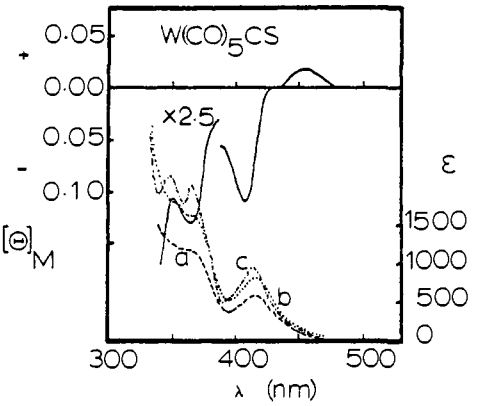

Figure 2. Optical and magnetic circular dichroism spectra of $W(CO)_5CS$: (a) MCD and optical spectra in dichloromethane at 300 K; (b) in alcohol (a commercial alcohol mixture of fluoromethyl, isopropyl, and ethyl alcohols was used) at 300 K; (c) in alcohol (see (b)) at 77 K (uncorrected for volume contractions).

Table II. Luminescence Data for $W(CO)_5L$ Complexes at 77 K

$W(CO)_5L$ L	cation	solvent	emission max, μm^{-1}	width at ½ height, μm^{-1}	lifetime, μs
Cl^-	PPN^+	alcohol[a]	2.010		15.8 ± 0.9
Cl^-	$AsPh_4^+$	2-Me-THF[b]	2.010	0.201	
Br^-	NEt_4^+	2-Me-THF[b]	2.014	0.256	13.4 ± 0.7
Br^-	$AsPh_4^+$	alcohol[a]	1.860	0.198	11.6 ± 0.5
I^-	PPN^+	alcohol[a]	1.802	0.179	15.1 ± 1.4
NCO^-	$AsPh_4^+$	2-Me-THF[b]	2.016	0.111	15.5 ± 1.2
N_3^-	$AsPh_4^+$	2-Me-THF[b]	1.945	0.145	10.6 ± 1.0

[a] 4:1 v/v EtOH–MeOH. [b] Complex suspended in the solvent.

+1 V causes a second oxidation to occur which deactivates the Pt bead working electrode, presumably through deposition of a decomposition product upon the electrode surface. Similar results are observed when the complex is reduced at a potential exceeding −1.5 V. In both cases, after the electrode surface is washed with concentrated HNO_3 the original plots are reproduced.

Table IV lists the potentials of the one-electron oxidations of these complexes. The latter three potentials have been reported for tungsten carbonyl pyrazine complexes where the lowest energy excited states are MTLCT.[17] Removal of an electron from $W(CO)_5X^-$ forms a neutral species, whereas the same reaction in the neutral pyrazine complexes results in the formation of a cation. The former reaction is favored and a lower potential is thus observed.

3. Photochemistry of the Halopentacarbonyltungstenate(0) Systems. When their lowest energy excited state was populated, the complexes $W(CO)_5X^-$ (X = Br, I, and NCO) exhibited low-efficiency ligand substitution photochemistry. For these ionic systems, temperature, cation, solvent, and wavelength effects on the quantum yields were observed. The chloropentacarbonyltungstenate ion underwent a rapid thermal ligand exchange reaction even in chloroform at −7 °C and therefore an accurate quantum yield could not be determined.

Irradiation of the ethylammonium or bis(triphenylphosphine)iminium (PPN) salts of $W(CO)_5X^-$ in carbon monoxide saturated chloroform solutions at either 436 or 405 nm resulted in the disappearance of the 400-nm feature in the UV/visible spectrum with an increase in intensity in the region $\lambda < 350$ nm. An isosbestic point was observed in the vicinity of 350–375 nm. The infrared spectra of the photolytes showed the disappearance of the three-band C_{4v} carbonyl pattern and the increase of the 1985-cm^{-1} $W(CO)_6$ T_{1u} band. The same changes were observed for the class 1 photochemical reactions.[4] The exclusive production of $W(CO)_6$, as indicated by the infrared spectra and the presence of isosbestic points in the UV/visible spectra, indicated that the only photoproduct under these conditions was $W(CO)_6$. The quantum yields for these unique ligand photosubstitution reactions are presented in Table V. For all three $W(CO)_5X^-$ ions, the efficiency of this reaction was considerably less than either the class 1 or 2 amine or phosphine complexes.[4] Furthermore, for the bromide material, a wavelength dependence was noted wherein the efficiency of the unique ligand photosubstitution was higher when the major low-energy spectral feature was irradiated at 405 nm than the efficiency when the red shoulder of this band was irradiated at 436 nm under identical conditions.

Table V also contains information concerning the carbonyl photosubstitution process. Photolysis of $[NEt_4][W(CO)_5Br]$ in pure acetonitrile did not lead to any detectable formation of the carbon monoxide photosubstitution product, $W(CO)_4(AN)(Br)^-$.[4] When $W(CO)_5I^-$ was photolyzed in a 0.1 M PPh_3 solution, only the monosubstituted product was detected in the infrared spectrum. A well-defined isosbestic point was observed in the UV/visible region during the initial stages of the reaction. A disubstituted product was a minor constituent of the photolysis mixture when the isocyanate complex was photolyzed in 1-propanol. Together these data indicate that the quantum yield for CO loss is much smaller than that for unique ligand loss in this series of materials.

Table III. $\nu_{(CO)}$ Infrared Data for the $W(CO)_5L$ Complexes[d]

$W(CO)_5L$ L	$A_1^{(1)}$, cm^{-1}	$A_1^{(2)}$, cm^{-1}	E, cm^{-1}	k_1(trans), mdyn/Å	k_2(cis), mdyn/Å	k_i, mdyn/Å	$\Delta\sigma$, mdyn/Å	$\Delta\pi$, mdyn/Å
Cl^- [a]	2069	1842	1922	13.82	15.67	0.37	1.02	−1.10
Br^- [a]	2071	1844	1924	13.85	15.70	0.37	1.05	−1.10
I^- [a]	2068	1850	1926	13.94	15.70	0.36	0.96	−1.01
NCO^- [a]	2069	1843	1921	13.84	15.66	0.38	0.98	−1.07
N_3^- [b]	2084	1849	1922	13.95	15.74	0.41	1.03	−1.04
CS[c]	2097	2008	1989	16.45	16.51	0.27	0.07	0.69
$C(CH_3)(OCH_3)$[c]	2073	1961	1938	15.73	15.83	0.34	−0.57	0.65
$C(Ph)(OCH_3)$[c]	2073	1961	1944	15.71	15.90	0.32	−0.41	0.56

[a] $CHCl_3$ solvent. [b] Taken from ref 5, $CHCl_3$ solvent. [c] Taken from ref 4, cyclohexane solvent. [d] For the anionic complexes the vibrational energies are insensitive to the nature of the cation.

Table IV. One-Electron Oxidation Potential vs. SCE of $W(CO)_5L$[a]

$W(CO)_5L$	$(\epsilon_p)_a$, V vs. SCE	$W(CO)_5L$	$(\epsilon_p)_a$, V vs. SCE
NCO^- [a]	0.628	pyridazine[b]	1.04
Br^- [a]	0.675	pyrazine[b]	1.04
I^- [a]	0.606	pyrimidine[b]	1.04

[a] Obtained in deoxygenated CH_2Cl_2 solution containing 0.01 M $[NBu_4][PF_6]$. [b] Obtained in deoxygenated CH_2Cl_2 solution containing 0.01 M $[NBu_4][ClO_4]$. Reference 19.

The effects of temperature on the unique ligand substitution yields are given in Table V. For the systems studied, an increase in temperature resulted in an increased rate of photosubstitution. Because the $W(CO)_5X^-$ systems were photolyzed at reduced temperatures (in comparison to the work on the amine and phosphine complexes)[4] in order to reduce interferences from thermal reactions, the lower temperature could have accounted for the reduced efficiency of substitution. At −6 °C, however, the unique ligand photosubstitution quantum efficiency of the class 1 $W(CO)_5NH_3$ complex still far exceeded that observed for the isocyanate and bromide materials indicating that there was a true reduction in efficiency for this reaction in the latter complexes. For $W(CO)_5I$, however, the unique ligand substitution efficiency at −6 °C was very similar to that observed for the class 1 amine compound, indicating that for $W(CO)_5I^-$ the photochemical behavior approaches that of the class 1 reactivity pattern.

The quantum efficiencies of the photochemical reactions of $W(CO)_5Br^-$ varied by over 300% when the Li^+, NEt_4^+, and $AsPh_4^+$ salts were irradiated in their lowest energy absorption feature at 436 nm. Not only was the formation yield of $W(CO)_6$ affected by changing the cation, but the presence of $AsPh_4^+$ substantially depressed the formation of the hexacarbonyl and a new dominant photoproduct occurred. This effect was observed in the isocyanate and azide systems as well as with the bromide material.[20]

Variation of the solvent also resulted in a marked effect on the quantum yield for unique ligand labilization. Even though the quantum yield of disappearance of the $W(CO)_5N_3^-$ system increased with temperature, this yield was lower in methanol at 7 °C than in $CHCl_3$ at −6 °C. In the other systems under the same conditions of cation and temperature, changing the solvent resulted in a change in the disappearance quantum yield. Furthermore, when 1-propanol was used as a solvent, the grow in of low-energy UV/visible features during photolysis indicated that disubstituted products were formed in which the alcohol acts as a ligand. There is no simple correlation between the quantum yields and either the solvent basicity or dielectric constant.

As noted in Table V, irradiation into the lowest energy excited state of the $AsPh_4^+$ salts of $W(CO)_5X^-$ resulted in reduced yields for the production of $W(CO)_6$. The efficiency of the reactant disappearance was undiminished, indicating that a new photoproduct was produced by the introduction of $AsPh_4^+$. During photolysis of these materials, all bands in the carbonyl region of the infrared spectrum disappear at the same rate as the major electronic spectral feature (~400 nm). Upon prolonged irradiation, all activity in the carbonyl infrared and electronic absorption at $\lambda > 250$ nm ceased and a white precipitate was observed in the photolyte. The rate of disappearance of the coordinated carbonyl bands in the infrared was the same as that of the $AsPh_4$ cation vibration at 1187 cm^{-1}. Quantitative analysis of the precipitate indicated that it contained As and W.

Qualitatively similar results occurred over a period of several hours if a deoxygenated $CHCl_3$ solution of $W(CO)_5X^-$ was allowed to stand in the dark. This disappearance was accelerated to the time scale of several minutes if a small quantity of benzoyl peroxide (a radical initiator and strong oxidant), Cl_2 gas, or phosgene was added to the solution. Over a period of months, a similar degradation appeared in the solids which were stored under N_2 in the dark. Because this decomposition product has no coordinated carbon monoxide, it is evident that it is the end result of a complex chain of reactions leading from some unstable initial product generated either thermally or photochemically and therefore further characterization of this material was not attempted. Because the final isolated product of this reaction is so far removed from the initial photogenerated species, this reaction was not investigated further. The initial step may be similar to the oxidative addition reaction of $AsPh_4^+$ to $Mn(CO)_5^-$.[19]

Discussion

1. Lowest Energy Excited State of $W(CO)_5X^-$ Complexes. In order to understand the class 3 reactivity pattern it is necessary to identify the character of the lowest energy excited state as either ligand field or charge transfer. In the class 1 and 2 amine and phosphine derivatives the lowest energy excited state has been assigned as LF, $^1A_1 \rightarrow E_{(T_{1g})}$.[4,7,11] Alternatively, in the isoelectronic $Mn(CO)_5X$ (X = halide) complexes, a ligand to metal charge transfer (LTMCT) state is lowest in energy.[20,21]

The MCD of the major band between 2.44 and 2.50 μm^{-1} in these $W(CO)_5X^-$ compounds (as exemplified by the spectrum of $W(CO)_5Br^-$ in Figure 1) is a positively signed Faraday *A* term. These MCD spectra are superimposable on that of $W(CO)_5N_3^-$.[5] Following the analyses of the MCD of the azide complex, two conclusions can be drawn. First, the transition involved is $^1A_1 \rightarrow E$. Second, the LUMO populated is the metal d_{z^2}. Also, as was stressed in the previous report of $W(CO)_5N_3^-$ spectroscopy,[5] the orbital origin of the transition (from either the metal d_{xz},d_{yz} or the ligand p_π orbitals) may not be determined from MCD spectroscopy.

Both the electronic absorption and emission spectra of these $W(CO)_5X^-$ complexes are inconsistent with a charge transfer assignment. If the electronic transition originated or termi-

Table V. Photochemical Quantum Yields for $W(CO)_5X^-$ Complexes

$W(CO)_5L$ L	cation	solvent	temp, °C	wavelength, nm	entering ligand[a]	photoproduct	$\phi_{disappearance}$[b]	$\phi_{app\ of\ prod}$[c]
Br^-	NEt_4^+	$CHCl_3$	7	436	CO	$W(CO)_6$	0.0034	0.0034
Br^- [g]	NEt_4^+	$CHCl_3$	7	405	CO	$W(CO)_6$	0.012	0.012
Br^- [g]	NEt_4^+	AN	7	405	AN	$W(CO)_5(AN)Br^-$		*d*
Br^- [h]	Li^+	$CHCl_3$	7	436	CO	$W(CO)_6$	0.094	0.094
Br^-	$AsPh_4^+$	$CHCl_3$	7	436	CO	$W(CO)_6$ + precipitate[f]	0.014	0.002[e]
I^-	PPN^+	$CHCl_3$	−6	436	CO	$W(CO)_6$	0.070	0.070
I^-	PPN^+	$CHCl_3$	−6	436	PPh_3[.1M]	$W(CO)_5PPh_3$	0.0040	0.0040
NCO^-	$AsPh_4^+$	$CHCl_3$	−6	436	CO	$W(CO)_6$ + precipitate[f]		0.0[e]
NCO^-	PPN^+	$CHCl_3$	−6	436	CO	$W(CO)_6$	0.009	0.009
NCO^-	PPN^+	$CHCl_3$	29	436	CO	$W(CO)_6$	0.020	0.020
NCO^-	PPN^+	acetone	−6	436	CO	$W(CO)_6$	0.050	0.050
NCO^-	PPN^+	1-propanol	−6	436	CO + 1-propanol	$W(CO)_6$ + disubstituted products		0.064
N_3^-	$AsPh_4^+$	$CHCl_3$	7	436	CO	precipitate[f]	0.071	0.0[e]
N_3^-	$AsPh_4^+$	MeOH	7	436	CO	precipitate[f]	0.037	0.0[e]
N_3^-	$AsPh_4^+$	Me_2SO	7	436	CO	precipitate[f]	0.018	0.0[e]
N_3^- [i]	PPN^+	$CHCl_3$	−6	436	CO	$W(CO)_6$ + $W(CO)_5NCO^-$	0.027	
N_3^- [i]	PPN^+	MeOH	7	436	CO	$W(CO)_6$ + $W(CO)_5NCO^-$	0.016	
NH_3		$CHCl_3$	−6	436	CO	$W(CO)_6$	0.064	0.064
NH_3		$CHCl_3$	7	436	CO	$W(CO)_6$	0.20	0.20
NH_3 [g]		$CHCl_3$	29	436	CO	$W(CO)_6$	0.50	0.50

[a] CO is at saturation. [b] Calculated for the disappearance of the $W(CO)_5L$ ligand field band error = ±15%. [c] Error = ±15% for Beer's law plots in the infrared. [d] Yield of disubstituted product is $<6 \times 10^{-3}$. [e] Yield for formation of $W(CO)_6$ only. [f] White arsenic containing precipitate formed upon photolysis. [g] Reference 4. [h] Reference 20. [i] Reference 5.

nated in an orbital which was principally "halogen" in character, the energy of this transition from one complex to another would vary as the difference in the optical electronegativities of the unique ligand (i.e., compared to the chloride complex, the lowest energy LTMCT transition in the bromide and iodide complexes should be red shifted 0.47 and 1.04 μm^{-1}, respectively).[22] Examination of the data in Tables I and II indicates that both the energies of absorption and emission are not nearly this sensitive to X.

The electrochemical results are consistent with the metal d_{xz},d_{yz} orbitals as the HOMO in these $W(CO)_5X^-$ complexes. The trends in the oxidation potentials follow the π-donor ability of the unique ligand, X, as assessed by both the Graham $\Delta\pi$ (Table III) and the known spectrochemical π-donor abilities for the halides.[23] From Table IV, the most easily oxidized complex, $W(CO)_5I^-$, has the best π-donor ligand while the Br^- complex has the worst π-donor ligand and is easily oxidized. This trend does not follow the optical electronegativities of the ligands.[22] Note that the lower oxidation potentials for $W(CO)_5X^-$ compared to $W(CO)_5$(pyrazine) are evidence for a larger amount of charge induced on the metal in the former complexes.

The infrared analysis of the anionic complexes indicates that these "halide" ligands are strong π donors when compared to ligands which give rise to class 1 and 2 photochemistry. The Graham $\Delta\sigma$ and $\Delta\pi$ parameters suggest that this results from the shifting of charge density from the "halide" p_π orbitals to the metal d_δ levels making more electron density available for dative metal-carbonyl π interactions and thus lowering the carbon-oxygen bond orders. This interpretation necessitates a good overlap and energy match-up of the metal and halide π orbitals thus further supporting the hypothesis of low-energy LTMCT states.

Semiquantitative energy considerations support the conclusions above. The Jørgensen optical electronegativity parameters for these halide and pseudohalide ligands follow: Cl, 3.0; Br, 2.8; I, 2.5; NCO, 3.0; N_3, 2.8.[22] The PES of $Mn(CO)_5Br$ indicated that the HOMO is primarily Br p_π in character with an ionization energy of 8.86 eV.[24] The PES of $W(CO)_6$ showed that the HOMO is a metal 5d orbital at 8.56 eV.[25] If the energies of these ligand π^* orbitals are taken as approximately equal to the energy of the Br π^* levels in

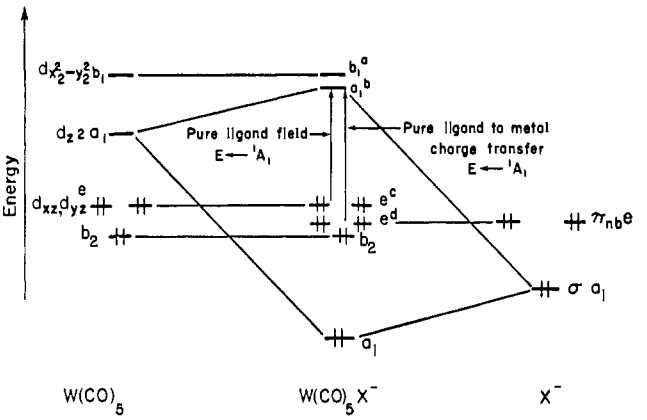

Figure 3. A one-electron molecular orbital diagram for the $W(CO)_5X^-$ ions. The metal-ligand bonding character of the orbitals follows: (a) metal-CO σ antibonding in the *xy* plane; (b) metal-X and metal-CO σ antibonding along the unique axis; (c) metal-X π antibonding; (d) metal-CO π bonding principally along the unique axis.

$Mn(CO)_5Br$ on the basis of the similarity of their electronegativities, the HOMOs of these $W(CO)_5X^-$ complexes are almost certainly not primarily ligand-centered orbitals. The increased charge on the tungsten center in these anionic complexes should raise the d-orbital energies relative to those in the manganese complex. The ligand π^* orbitals of e symmetry must be energetically close to the HOMO.

From these data it is concluded that the HOMOs in these $W(CO)_5X^-$ systems are the metal (d_{xz},d_{yz}) orbitals and that the LUMOs are metal d_{z^2}. The variation of the oxidation potentials indicates that the "halide" orbitals are energetically close to the metal π orbitals (d_{xz},d_{yz}). These conclusions provide the basis for construction of a one-electron molecular orbital diagram for these systems as in Figure 3. The relative bonding properties of each orbital have been noted in the figure caption.

2. Lowest Energy Excited State in $W(CO)_5CS$. The lack of a low-energy *A* term in the MCD spectrum of $W(CO)_5CS$ (Figure 2) necessitates that the lowest energy electronic transition in this material does not terminate in a degenerate electronic level. This observation confirms our previous as-

signment of the lowest unoccupied molecular orbital in this CS material as the e CS π^* level.[4] Therefore, the lowest energy transition is the e (d_{xz},d_{yz}) → e (CS π^*) giving rise to the manifold of states, A_1, A_2, B_1, and B_2. The transition to the A_1 state is fully dipole allowed. None of these states are degenerate (the necessary condition for observation of a MCD *A* term) and consequently only *B* terms are observed. A similar assignment was proposed for the carbene complexes of $W(CO)_6$.[4]

The infrared analysis of $W(CO)_5L$ (L = CS and carbenes) indicates that these ligands are much stronger than the amines or halides and approach the ligand field strength of CO. The absence of a low-energy *A* feature in the MCD of $W(CO)_5CS$ indicates that the LF state which gives rise to this feature is shifted to higher energy regions as is expected for the CS ligand. Therefore, the low-energy bands in these three materials (Table I) are MTLCT transitions and excitation in the region of 400 nm will not populate any ligand field type states. Luminescence from the MTLCT state in the CS and carbene derivatives could not be detected.

3. Photochemistry. Previously the class 3 designation was established for complexes where all modes of ligand photosubstitution proceed with an efficiency less than $\sim 10^{-2}$ and was attributed to charge transfer character in the lowest energy excited state.[4] The anionic $W(CO)_5X^-$ derivatives also exhibit low-efficiency photochemistry but have primarily LF character in their lowest excited states. Thus, for the compounds which have now been reported, two subclasses of class 3 reactivity emerge. The ionic materials behave like class 1 compounds (predominantly unique ligand loss with reduced CO substitution) but at a lower overall efficiency. This pattern of inefficient unique ligand photosubstitution with even less efficient carbonyl labilization, as shown in the reactions

class 3(1) reactions

$$W(CO)_5L + L' \xrightarrow{h\nu\ \phi_1} W(CO)_5L' + L \qquad (1)$$

$$W(CO)_5L + L' \xrightarrow{h\nu\ \phi_2} W(CO)_4LL' + CO \qquad (2)$$

$$L = Br^-, I^-, NCO^-$$

$$\phi_1 \simeq 10^{-2};\ \phi_2 \simeq 10^{-3}$$

will be referred to as class 3(1). Secondly, the reactivity of the CS and carbene complexes is similar to reduced class 4 photochemistry (predominant CO loss with inefficient L loss) and will be labeled class 3(2). Reactions 3 and 4 outline these photochemical reactivity patterns.

class 3(2) reactions

$$W(CO)_5L + L' \xrightarrow{h\nu\ \phi_1} W(CO)_5L' + L \qquad (3)$$

$$W(CO)_5L + L' \xrightarrow{h\nu\ \phi_2} W(CO)_4LL' + CO \qquad (4)$$

$$L = CS, C(CH_3)(OCH_3), C(Ph)(OCH_3)$$

$$1 \gg \phi_2 > \phi_1$$

The observed subclassification of 3(1) photochemistry for the $W(CO)_5X^-$ compounds could have been the result of the charge on the complex affecting the reaction mechanism. Two observations eliminate the possibility that the reduced efficiencies are a simple consequence of the charge. First, photolysis of $[AsPh_4][W(CO)_5CN]$ at 405 nm in CO-saturated $CHCl_3$ at −10 °C results in photodecomposition with a quantum yield approaching unit.[26] Second, photolysis of anionic $M(CO)_6^-$ (M = V, Nb, and Ta) in the presence of an entering ligand leads to photosubstitution products with a yield in excess of 60%.[27]

In the cyanide complex, the bonding properties of the cyanide ligand are radically different from those of the halide and pseudohalide ligands under consideration here. That photodecomposition occurs with very high quantum efficiency in this material indicates that the presence of a unit negative charge on the reactant is not of itself responsible for the reduced yields observed for the other $W(CO)_5X^-$ materials.

4. A Bonding Model of the Origins of Class 3(1) and 3(2) Photochemistry. The reduced efficiencies of the class 3(1) $W(CO)_5X^-$ compounds may be explained in terms of the increase in π bonding in the excited state. The relevant diagram for the anionic complexes is presented in Figure 3. In this strong field picture, population of the lowest energy excited state in the anionic class 3(1) materials, the LF $E_{(T_{1g})}$ state, corresponds to population of the d_{z^2}, axially σ antibonding orbital and depopulation of the d_{xz},d_{yz} metal-"halide" π antibonding and metal-CO π bonding level. Alternatively, in the LTMCT state, the d_{z^2} orbital is still occupied. In this case, however, the electron is removed from the metal-"halide" π-bonding level.

The empirical observations of the photochemistry exhibited by these complexes demonstrates the relative importance of σ- and π-bonding alterations in highly covalent systems. Considering only the metal-unique ligand bond, there is a large decrease in the net σ bond order and an increase in the π bond order in the $E_{(T_{1g})}$ state. Hence, the total substitutional efficiency of this bond in the LF excited state is reduced relative to the same reaction in the amine or phosphine derivatives.[4] In these later cases, the d_{xz},d_{yz} "metal" orbitals which are depopulated are either nonbonding or π bonding with respect to the metal-unique ligand linkage. Thus, a strengthening of π interactions, even in the presence of a large reduction of σ bonding, will result in a lowering of the quantum efficiency of ligand substitution.

This conclusion is further supported by the photochemistry of $W(CO)_5I^-$ and the wavelength dependence of $W(CO)_5Br^-$. When $W(CO)_5Br^-$ is irradiated at 405 nm rather than 436 nm, more energy is placed in the LTMCT state which lies at slightly higher energy than the LF state. For $W(CO)_5I^-$ (iodine has the lowest optical electronegativity of any of the ligands studied) the LTMCT is expected to lie much closer to or equal to the energy of the LF state. Hence 435-nm photolysis will cause more population of the LTMCT state in this compound than in the others. In both cases, the halide photosubstitution yield rises to approach that of class 1 reactivity. In the LTMCT state, rather than depopulating the metal-halide π antibonding orbital, the metal-X^- π-bonding level is vacated thus resulting in a decrease in both the π and σ M-X bond order. This decrease leads to an increase in the substitutional lability of this bond.

Finally, the low efficiency of carbonyl photosubstitution must be considered. As has been mentioned previously, the large negative values of $\Delta\pi$ and the very low carbon-oxygen force constants (Table III) observed in these $W(CO)_5X^-$ materials are indicative of the large negative charge centered on the metal which results in a very high degree of metal to carbon monoxide back-bonding and high metal-carbon bond orders in the ground state. Consistent with the model developed for class 1 and 2 materials,[4] if a metal-carbonyl bond is of high order in the ground state, even very anisotropic σ antibonding in the excited state will not lead to a high substitution yield for this bond.

The previously reported photochemical activities of substituted pyridine derivatives of tungsten hexacarbonyl[6] fall into the class 3(1) assignment. This reactivity pattern is interpreted as arising from direct population of the low-energy LF state which is beneath the MTLCT absorptions in these complexes. The reduction in overall efficiency occurs because the large MTLCT band receives most of the excitation energy and acts

as an internal filter of the LF feature. When there is a low-lying LF state to receive direct population upon low-energy photolysis, as in the CS and carbene systems where the LF state is much higher in energy than the MTLCT state at ~400 nm, reduced M-CO and M-L (class 3(2)) reactivity is observed.

5. Luminescence Phenomena. The qualitative similarity of the emission spectra of the class 3(1) complexes and the class 1 and 2 complexes previously studied[4,14] suggests that emission occurs from the LF excited state. Where this state is not populated, as in the class 3(2) materials, no emission is detected implying that the pure MTLCT state does not emit. The absence of emission may result from rapid nonradiative decay of the MTLCT state. Rapid nonradiative and nonreactive decay would also offer an explanation of the reduced photoreactivity.

The trend in the luminescence lifetimes, (class 1 and 2) < "halide" derivatives (class 3(1)) < substituted pyridine complexes (class 3(1)), parallels the total ligand substitution photoreactivity of these materials. The more photoactive complexes have shorter lifetimes. A recent molecular orbital calculation of the coordinatively unsaturated $Cr(CO)_5$ species in various geometries indicated that the excited state of $M(CO)_5$ correlates with a ground electronic state by rearrangement from a square pyramid to a trigonal bipyramid.[28] Therefore, this nonradiative decay path to the ground state is more important for those materials which demonstrate efficient ligand photosubstitution (ammine and phosphine derivatives) than for those with reduced photochemical efficiency ("halides" and substituted pyridine complexes). This increase in nonradiative deactivation may account for the shorter lifetimes of these class 1 and 2 materials in comparison to the class 3(1) and 3(2) complexes.

6. Conclusions. Class 3 photochemical reactivity of $W(CO)_5L$ complexes may be subdivided into two subclasses, 3(1) and 3(2). Class 3(1) photochemistry results from irradiation of a lowest energy excited state which is ligand field in character. The reduction in photoactivity arises due to either increases in metal-L π interactions upon attaining the excited state or from inner filtering by overlapping charge transfer transitions as in the cases of substituted pyridine complexes. Class 3(2) photochemistry is characteristic of a MTLCT state in which M-L σ antibonding orbitals are not populated.

Experimental Section

1. Preparation and Characterization of Compounds. All materials were prepared by modification of literature methods in freshly distilled solvents under nitrogen. Photolysis was conducted in an Ace photochemical immersion well equipped with a Hanovia 550-W UV source.

$W(CO)_5NH_3$. $W(CO)_6$ (1.36 g) was irradiated in 100 mL of THF for 2 h with constant N_2 purge. After photolysis, anhydrous NH_3 gas was passed through the yellow solution producing a yellow precipitate which was collected by filtration. Sublimation at 50 °C (1 mm) for several hours removed residual $W(CO)_6$. The yellow residue was twice recrystallized from 1:1 (v/v) hexane–ether. Anal. Calcd for $WC_5O_5NH_3$: C, 17.60; H, 0.89. Found: C, 18.00; H, 0.99.

[$AsPh_4$][$W(CO)_5N_3$].[29] Anal. Calcd for $WC_{29}H_{20}O_5N_3As$: C, 46.48; H, 2.70; W, 24.54; N, 5.61. Found: C, 46.22; H, 2.57; W, 24.80; N, 4.89. Reported carbonyl IR[29] (cm^{-1}): 2076, 2040 (N_3), 1914, 1853. Found: 2084, 2048 (N_3), 1922, 1849 ($CHCl_3$ solution).

[PPN][$W(CO)_5N_3$]. $W(CO)_6$ (1.00 g) was irradiated for 1.5 h in 100 mL of THF under constant N_2 purge. [PPN][N_3] (0.45 g) in 50 mL of acetone was added to this yellow solution at room temperature and it was immediately rotoevaporated to a yellow oil at 35 °C. The oil was suspended in 20 mL of EtOH, filtered, and rotoevaporated. The residue was dissolved in 25 mL of boiling EtOAc which was slowly cooled to 0 °C producing a light yellow precipitate. The yellow solution was decanted into 150 mL of pentane, forming an oil on the bottom of the vessel. The oil [PPN][$W(CO)_5N_3$] was washed with additional pentane and vacuum dried for 2 days resulting in a solid containing 5% $W(CO)_6$ as an impurity. Carbonyl IR (cm^{-1} in $CHCl_3$): 2084, 2049 (N_3), 1985 ($W(CO)_6$), 1922, 1849.

[Li]- and [Na][$W(CO)_5N_3$] were prepared by addition of a stoichiometric amount of the azide salt in 25 mL of MeOH to a solution of 0.25 g of $W(CO)_6$ in 25 mL of THF irradiated as described above. The solution was rotoevaporated to 5 mL, filtered, and eluted down a 1-ft silica gel column with $CHCl_3$. The first yellow band was collected. IR bands (cm^{-1}) at 2084, 2049 (N_3), 1922, and 1855 confirmed the presence of $W(CO)_5N_3^-$.

[$N(Et)_4$][$W(CO)_5Br$].[30] Anal. Calcd for $WC_{13}O_5H_{20}NBr$: C, 29.23; H, 3.78. Found: C, 29.44; H, 3.93. Carbonyl IR in KBr disk (cm^{-1}): 2072, 1923, 1893. IR in $CHCl_3$ (cm^{-1}): 2071, 1924, 1844.

[Li][$W(CO)_5Br$]. A solution of 2.00 g of $W(CO)_6$ in 100 mL of THF was irradiated for 2 h under a constant N_2 purge. To this yellow solution was added 1 g of LiBr dissolved in 50 mL of MeOH. The volume of the solution was reduced to 25 mL under vacuum. This solution was filtered, placed on a 1-ft silica gel column, and eluted with $CHCl_3$. The yellow band was isolated and this procedure was repeated three times resulting in a $CHCl_3$ solution containing [Li][$W(CO)_5Br$] which was identified by infrared absorptions at 2071, 1846, and 1924 cm^{-1}. The concentration was adjusted by evaporation of the solvent and determined from the absorption of the $W(CO)_5Br^-$ ion at 400 nm in the visible spectrum.

[$AsPh_4$][$W(CO)_5Br$]. To a $CHCl_3$ solution of [Li][$W(CO)_5Br$] prepared as described above was added 1 g of $AsPh_4Cl{\cdot}H_2O$ dissolved in 25 mL of EtOH. The $CHCl_3$ was eliminated from this material by rotary evaporation resulting in a deep yellow EtOH solution. The product was precipitated from this solution by the slow addition of water and was collected by filtration and washed with an additional 50 mL of water. Carbonyl IR (cm^{-1}) in $CHCl_3$: 2071, 1843, 1924.

$W(CO)_5CS$.[31] Repeated crystallization from pentane was used to purify the material. After five recrystallizations the substance was judged to contain less than 1.5% $W(CO)_6$ as an impurity based on the carbonyl IR spectrum. Reported carbonyl IR (cm^{-1}): 2096, 2007, 1989. Found: 2097, 2008, 1989.

[$AsPh_4$][$W(CO)_5Cl$]. A 100-mL diglyme solution containing 2.00 g of $W(CO)_6$ and 0.25 g of LiCl was refluxed for 12 h under N_2, resulting in a black mixture. Upon cooling and filtering, a yellow liquid was obtained to which 200 mL of pentane was added. This material was cooled to −40 °C, which resulted in the separation of a green oil. The light yellow diglyme/pentane phase was decanted, 50 mL of EtOH containing 2.00 g of $AsPh_4Cl{\cdot}H_2O$ was added to the oil, and the resultant solution was filtered. Water was slowly added to the filtrate which caused the product to precipitate as bright yellow crystals which were collected, washed, and vacuum dried. Anal. Calcd for $WC_{29}H_{20}O_5ClAs$: C, 46.89; H, 2.72. Found: C, 44.34; H, 2.65. Carbonyl IR (cm^{-1}) in $CHCl_3$: 2069, 1842, 1922.

[PPN][$W(CO)_5I$]. A solution of 1.00 g of $W(CO)_6$ and 0.6 g of $LiI{\cdot}4H_2O$ in 50 mL of diglyme was heated to 100 °C under N_2 and stirred for 12 h, resulting in a dark green solution. After the solution was cooled to 35 °C and filtered, 1.60 g of [PPN][Cl] dissolved in 25 mL of diglyme was added to the yellow filtrate which was again filtered. Medium-range petroleum ether was slowly added to this clear, yellow solution until a yellow precipitate formed which deposited on the bottom of the flask as an oil. Repeated washing of this oil with petroleum ether resulted in the formation of a solid material. This solid was dissolved in 25 mL of EtOH and addition of water caused the product to reprecipitate. These bright yellow crystals were collected by filtration, washed with petroleum ether, and dried in vacuo. Anal. Calcd for $WC_{41}O_5IH_{30}P_2N$: C, 49.77; H, 3.66. Found: C, 48.37; H, 2.99. Carbonyl IR (cm^{-1}) in $CHCl_3$: 2068, 1850, 1926.

[$AsPh_3$][$W(CO)_5NCO$].[32] Anal. Calcd for $WC_{30}H_{20}O_6NAs$: C, 48.09; H, 2.70; N, 1.87. Found: C, 47.73; H, 2.48; N, 1.58. Reported carbonyl IR[32] (cm^{-1}): 2230 (NCO), 2062, 1915, 1854 (acetone). Found: 2236 (NCO), 2069, 1921, 1843 ($CHCl_3$).

[PPN][$W(CO)_5NCO$]. [PPN][$W(CO)_5N_3$] (0.5 g) was refluxed in 100 mL of CO-saturated EtOH for 1 h, after which the volume of the solution was reduced to 10 mL and the solution was cooled to room temperature. The product was precipitated by the slow addition of H_2O and collected by filtration followed by several water washes. Anal. Calcd for $WC_{24}H_{30}N_2P_2O_6$: C, 55.77; H, 3.35; N, 3.10; W, 20.33. Found: C, 54.60; H, 3.36; N, 3.27; W, 20.06. Carbonyl IR (cm^{-1} in $CHCl_3$): 2236 (NCO), 2069, 1921, 1843.

[PPN][Cl][33] was used to prepare [PPN][N_3] by metathesis.

2. Photochemistry. The methods for irradiation of the samples and determination of the quantum yields have been discussed previously.[4]

3. Electronic and Vibrational Spectra. Infrared spectra in the 4.5–5.65-μ region were obtained with a Beckman IR-4 instrument. In this region the 1985-cm^{-1} $W(CO)_6$ peak, which was a minor impurity in all of the samples, was used as a reference for the calibration of the band energies of the carbonyl stretching vibrations of the $W(CO)_5L$ materials. For those experiments in which quantitative IR absorptions were used to calculate the reactant and product concentrations, the instrument was calibrated with a set of standardized neutral density filters to establish the % T scale. A Perkin-Elmer 521 instrument was used for other infrared ranges.

Room temperature UV/visible spectra were recorded on Cary Model 11, 14, and 15 spectrophotometers in quartz cells. Liquid nitrogen temperature spectra were obtained with an exchange gas Dewar placed in the sample compartment of the Cary 14 instrument.

4. Magnetic Circular Dichroism Spectroscopy. The magnetic circular dichroism spectra were obtained by Professor A. F. Schreiner at North Carolina State University with a JASCO spectropolarimeter (ORD/UV/CD-5) and a high-field magnet.[34] The field was measured to within 1% accuracy with a Rawson-Lush gaussmeter.

5. Electrochemistry. The cyclic voltammetry experiment was conducted on an instrument constructed within the department. The working electrode was a Beckman platinum bead. The reference was a saturated calomel electrode with an agar salt bridge and a medium-porosity sinter isolating the aqueous solution from the nonaqueous electrolyte. An in-house fabricated platinum spiral auxiliary electrode was also used.

$W(CO)_5L$ solutions (25 mL, 10^{-3} M) in a base electrolyte consisting of 10^{-2} M [n-butylammonium][PF_6] in CH_2Cl_2 were deoxygenated in the electrochemical cell by vigorously bubbling N_2 through the solution. The solutions were allowed to become quiescent by resting for 15 min with a gentle stream of N_2 blown over the top before the voltammogram was obtained. A scan rate of 3 V/min was used and the scan was initially toward negative potentials.

6. Emission Spectroscopy. EPA and 4:1 EtOH–MeOH were not purified before use but were deoxygenated by bubbling N_2 through the solvents for approximately 15 min. 2-MeTHF was refluxed overnight over $CuCl_2$ and then triply distilled under N_2 from CaH_2 in order to remove luminescent impurities. Methylcyclohexane was distilled from P_2O_5 and deoxygenated by nitrogen purging. The spectra were obtained on a Spex Fluorolog instrument modified to accept a quartz Dewar.[4]

The luminescence lifetimes were obtained using 400-nm pulses of less than 2-ns duration from a Molectron N_2 dye laser for excitation. The emission was passed through a Jarrell-Ash 0.5-m monochromator tuned to 533 nm and detected with a 9502 (S response) PMT in a photon counting mode. The tube output was interrogated at 0.2-μs intervals after the flash by a high-speed digitizer slaved to a dedicated Biomation minicomputer. The intensity in each interval was averaged over several pulses in this computer and then sent to the departmental PDP 11/45 data processing system, where these values were stored in a disk file.

The comparison method for optically dilute solutions[35] was used to determine the luminescence quantum yields at 77 K on the Spex instrument for $W(CO)_5L$ (L = Br, NEt_4, and $AsPh_4$ salts, and py). The samples were in rigid glasses (either 2-MeTHF or 4:1 EtOH–MeOH). The emission was viewed at 90° to the excitation source which was collimated to 1 mm by a slit parallel to and centered with respect to the sample tube. The path length of the excitation beam through the sample was calculated to have been 4.78 mm. The band-pass of both the excitation and emission monochromators was set at 1 nm. Exactly the same conditions of optical train and geometry were utilized for the samples and the reference, which was $Ru(bpy)_3Cl_2 \cdot 6H_2O$ in a 4:1 EtOH–MeOH glass at 77 K. The quantum yield for this reference was taken as 0.376 ± 0.036.[36] The ratio of the light absorbed by the reference complex to that by the sample was determined by examining the room temperature absorption spectra in a 1-mm path on the Cary 14 instrument.

Four independently prepared samples of each of the compounds and of the reference were examined with the Spex and for each solution excitation and emission spectra were recorded. The relative emission intensity of the samples compared to the reference was determined by cutting and weighing the emission spectra. Quantum yields were calculated for nine excitation wavelengths between 350 and 430 nm using eq 16 of ref 35 for each solution. The experimental error was estimated to be ±20% from the standard deviation of these ϕ values. As the emission spectra of the reference and the compounds under investigation were very similar in energy, no corrections for the PMT response were applied. When the samples were in 2-MeTHF glasses, a refractive index correction was used.

Acknowledgments. We wish to thank Professor A. F. Schreiner for making the MCD spectra available to us. The support of the National Science Foundation is gratefully acknowledged.

References and Notes

(1) Presented in part at the Symposium on Inorganic Photochemistry, Joint Meeting of the ACS and SAS, Anaheim, Calif., Oct 1977, Paper 205.
(2) National Science Foundation National Needs Trainee, 1977–1978.
(3) Henry and Camille Dreyfus Foundation Teaching Scholar, 1974–1979.
(4) R. M. Dahlgren and J. I. Zink, *Inorg. Chem.*, **16**, 3154 (1977).
(5) R. M. Dahlgren and J. I. Zink, *Inorg. Chem.*, submitted for publication.
(6) M. Wrighton, *J. Am. Chem. Soc.*, **98**, 4105 (1976).
(7) M. Wrighton, *Inorg. Chem.*, **13**, 905 (1974).
(8) M. Wrighton, G. S. Hammond, and H. B. Gray, *Mol. Photochem.*, **5**, 179 (1973).
(9) D. M. Allen, A. Cox, T. J. Kemp, and L. H. Ali, *J. Chem. Soc., Dalton Trans.*, 1899 (1973).
(10) M. Wrighton, D. L. Morse, H. B. Gray, and D. K. Ottensen, *J. Am. Chem. Soc.*, **98**, 1111 (1976).
(11) A. Vogler, "Concepts of Inorganic Photochemistry/', A. W. Adamson and P. D. Fleischauer, Eds., Wiley-Interscience, New York, 1975.
(12) The MCD analysis has been preformed by Professor A. F. Schreiner, Department of Chemistry, North Carolina State University, Raleigh, N.C. 27607.
(13) R. M. Dahlgren, "The Photochemistry and Spectroscopy of Monosubstituted Derivatives of Tungsten Hexacarbonyl", Ph.D. Thesis, University of California, Los Angeles, 1978.
(14) (a) M. Wrighton, G. S. Hammond, and H. B. Gray, *J. Am. Chem. Soc.*, **93**, 4336 (1971); (b) *Inorg. Chem.*, **11**, 3122 (1972).
(15) F. A. Cotton and C. S. Kraihanzel, *J. Am. Chem. Soc.*, **84**, 4432 (1962).
(16) W. A. G. Graham, *Inorg. Chem.*, 7, 315 (1968).
(17) K. H. Pannell, M. Gonzales, H. Leano, and R. Iglesias, *Inorg. Chem.*, **17**, 1093 (1978).
(18) R. M. Dahlgren and J. I. Zink, *J. Chem. Soc., Chem. Commun.*, in press.
(19) R. A. Faltynek and M. S. Wrighton, *J. Am. Chem. Soc.*, **100**, 2701 (1978).
(20) R. M. E. Vliek and P. J. Zandstra, *Chem. Phys. Lett.*, **31**, 487 (1975).
(21) R. A. N. McLean, *J. Chem. Soc., Dalton Trans.*, 1568 (1974).
(22) C. K. Jørgensen, *Prog. Inorg. Chem.*, **12**, 101 (1970).
(23) A. B. P. Lever, *Coord. Chem. Rev.*, **4**, 73 (1969).
(24) D. L. Lichtenberger, A. C. Sarapu, and R. F. Fenske, *Inorg. Chem.*, **12**, 702 (1973).
(25) B. R. Higginson, D. R. Lloyde, P. Burroughs, D. M. Gibson, and A. F. Orchard, *J. Chem. Soc., Faraday Trans. 2*, **69**, 1659 (1973).
(26) R. M. Dahlgren, E. Bell, and J. I. Zink, unpublished results.
(27) M. S. Wrighton, D. I. Handeli, and D. L. Morse, *Inorg. Chem.*, **15**, 434 (1976).
(28) P. J. Hay, *J. Am. Chem. Soc.*, **100**, 2411 (1978).
(29) H. Werner, W. Beck, and H. Engelmann, *Inorg. Chim. Acta*, **3**, 331 (1969).
(30) E. W. Abel, I. S. Butler, and J. G. Reid, *J. Chem. Soc.*, 2068(1963).
(31) B. D. Dombek and R. J. Angelici, *J. Am. Chem. Soc.*, **95**, 7516 (1973).
(32) W. Beck, H. Werner, H. Englemann, and H. S. Smedal, *Chem. Ber.*, **101**, 2143 (1968).
(33) J. K. Ruff and W. J. Schlientz, *Inorg. Synth.*, **15**, 84 (1974).
(34) P. J. Hauser, A. F. Schreiner, and R. S. Evans, *Inorg. Chem.*, **13**, 1925 (1974).
(35) J. N. Demas and G. A. Crosby, *J. Phys. Chem.*, **75**, 991 (1971).
(36) J. N. Demas and G. A. Crosby, *J. Am. Chem. Soc.*, **93**, 2841 (1971).